

Recognition of objects in orbit and their intentions with space-borne sub-THz Inverse Synthetic Aperture Radar

Cherniakov, Mikhail; Hoare, Edward g.; Gashinova, Marina; Marchetti, Emidio; Stove, Andrew g.

DOI:

[10.1049/rsn2.12513](https://doi.org/10.1049/rsn2.12513)

License:

Creative Commons: Attribution (CC BY)

Document Version

Publisher's PDF, also known as Version of record

Citation for published version (Harvard):

Cherniakov, M, Hoare, EG, Gashinova, M, Marchetti, E & Stove, AG 2023, 'Recognition of objects in orbit and their intentions with space-borne sub-THz Inverse Synthetic Aperture Radar', *IET Radar, Sonar & Navigation*. <https://doi.org/10.1049/rsn2.12513>

[Link to publication on Research at Birmingham portal](#)

General rights

Unless a licence is specified above, all rights (including copyright and moral rights) in this document are retained by the authors and/or the copyright holders. The express permission of the copyright holder must be obtained for any use of this material other than for purposes permitted by law.

- Users may freely distribute the URL that is used to identify this publication.
- Users may download and/or print one copy of the publication from the University of Birmingham research portal for the purpose of private study or non-commercial research.
- User may use extracts from the document in line with the concept of 'fair dealing' under the Copyright, Designs and Patents Act 1988 (?)
- Users may not further distribute the material nor use it for the purposes of commercial gain.

Where a licence is displayed above, please note the terms and conditions of the licence govern your use of this document.

When citing, please reference the published version.


Take down policy

While the University of Birmingham exercises care and attention in making items available there are rare occasions when an item has been uploaded in error or has been deemed to be commercially or otherwise sensitive.

If you believe that this is the case for this document, please contact UBIRA@lists.bham.ac.uk providing details and we will remove access to the work immediately and investigate.

ORIGINAL RESEARCH

Recognition of objects in orbit and their intentions with space-borne sub-THz Inverse Synthetic Aperture Radar

Mikhail Cherniakov¹ | Edward G. Hoare¹ | Marina Gashinova¹ | Emidio Marchetti² | Andrew G. Stove¹ 

¹School of Electrical, Electronic and Systems Engineering, University of Birmingham, Birmingham, UK

²Continental Engineering Services, Burgess Hill, UK

Correspondence

Andrew G. Stove, 45 Mansfield Road, Hove BN3 5NL, UK.
Email: andystove@virginmedia.com

Funding information

Defence Science and Technology Laboratory, United Kingdom, Grant/Award Number: DSTLX1000163770

Abstract

An important aspect of Space Situational Awareness is to estimate the intent of objects in space. This paper discusses how discriminating features can be obtained from Inverse Synthetic Aperture Radar images of such objects and how these discriminators can be used to recognise the objects or to estimate their intent. If the object is, for example, a satellite of a known type, the scheme proposed is able to recognise it. The ability of the scheme to detect damage to the object is also discussed. The focus is on imagery obtained in the sub-terahertz band (typically 300 GHz) because of the greater imaging capability given by the diffuse scattering which is observed at these frequencies. The paper also discusses the importance of being able to use images obtained by electromagnetic simulation to be able to train the subsystem which recognises features of the objects and describes a practical scheme for creating these simulations for large objects at these very short wavelengths.

KEYWORDS

electromagnetic wave scattering, radar imaging

1 | INTRODUCTION

As the number of objects in orbit, and in particular satellites, increases and as we all come to depend more and more on the capabilities they offer, such as communications and Earth observation and others, it becomes more important that we have good awareness of the state and the intent of the satellites and other objects which are orbiting the Earth (Space Situational Awareness (SSA)). At the same time, the increasing number of these objects is also making that task harder. This paper uses the term ‘intent’ for what might otherwise be called the ‘purpose’ of the object since the former term is more closely aligned with the terminology used by military surveillance communities.

Large ground-based radars have historically been the backbone of SSA, providing high detection probabilities at long ranges and the ability to track several objects at one time. Examples of such radars are the German Tracking and Imaging Radar [1] and the radars in the US Space Surveillance

Network [2]. Since they are ground-based, they are best suited for observing objects in Low Earth Orbit (LEO). Since they are large and expensive, many different surveillance demands will compete for their finite resources of surveillance time and look direction. The reducing cost of satellite launches means that in coming years, space-borne radars [3, 4] might be at a lower cost for SSA than the use of ground-based assets, while their design will certainly be simpler.

The primary requirement, of course, has been to keep track of these objects, but a secondary aim is to understand their intent/purpose. Achieving this can greatly help if the satellite can be imaged, that is, if we can see its features its size, the arrangement of its solar panels, whether it deploys distinctive sensors (radars or telescopes) or large communications antenna, or other distinctive descriptors. This can currently be achieved using Inverse Synthetic Aperture Radar (ISAR), [5] but as mentioned above, the Earth-based imaging radars are very costly because of their large antennas and high transmitter powers, so there are only a few of them worldwide, and they do

This is an open access article under the terms of the [Creative Commons Attribution](https://creativecommons.org/licenses/by/4.0/) License, which permits use, distribution and reproduction in any medium, provided the original work is properly cited.

© 2023 The Authors. *IET Radar, Sonar & Navigation* published by John Wiley & Sons Ltd on behalf of The Institution of Engineering and Technology.

not have enough capacity to perform all the imaging which may be needed, and certainly not with the timeliness which will be required in the future. They are also only capable of imaging satellites in LEO, but not those in higher orbits.

An alternative is to put the imaging sensor in space, which is a subject of research on Space Domain Awareness. The authors in Refs. [6, 7] have shown that a compact ISAR system working at a frequency in the range around 100–300 GHz (sub-THz frequencies) is feasible which will image a satellite at a range of up to 100 km with centimetric resolution. The payload would be about 30 kg, with a volume of about 30 l, and it would thus be smaller and lighter than an optical system with similar resolution. The radar sensor will also be immune to dazzle from the sun and would operate during the eclipse of the object being imaged.

Using a space-based sensor also has the additional advantage that whereas a ground-based sensor can only image the aspect of an object as seen from Earth, the space-based sensor can potentially image the object from any aspect.

1.1 | Obtaining and using information

At the top level, the concept of the proposed radar system is the same as for other space surveillance systems: The system will have access to ephemeris data on the object and will obtain images of it which will be combined with other information, for example, the object's kinematics, to obtain the best estimate of its intent. The ISAR system also provides data on the internal rotation motion of the object, which may not be available from other sensors. The images are used for three purposes: firstly to obtain information on the object based on the sizes of the descriptors, such as estimating the power-generating capacity based on the size of the solar panels, and secondly to estimate its aspect, that is, to answer questions such as 'is its telescope pointing at the Earth or into space?' The third use is to use the set of descriptors seen on the object to make a deduction about the intent. The full system will combine all these types of data, but this paper will concentrate on the last activity—recognising the descriptors and obtaining an estimate of the object's intent from them.

1.2 | Inverse Synthetic Aperture Radar

The proposed radar uses the principle of ISAR imaging. This achieves the down-range resolution from the signal bandwidth in the usual way, but, of course, the cross-range resolution is obtained by measuring the differential Doppler shifts from different parts of the target as it rotates when crossing the radar's field of view. Even if the target has no internal rotation, unless it is travelling on a course exactly towards or away from the radar, it will appear to rotate as its aspect to the radar changes while it travels through the radar beam. The physical beamwidth of the radar is used to

prevent the detection of other objects at the same range as the target but in different directions. It also focuses the transmitted energy onto the target. The requirement for real-mode angular discrimination is quite modest in this application since the density of objects in space is sufficiently low that there will be few objects in other directions at the same range as the target.

The recognition of surface targets from ISAR images is often made more complicated by the fact that the motion of the target is not known, may involve rotation about many axes and is non-linear. The situation is much easier for objects in space: Their translational motion is generally ballistic, and over the timescales required for ISAR imaging, it can be considered linear. Many satellites do not have internal rotations, and for most of those that do, their motion is again quite simple. If the satellite is tumbling, the Doppler processing can also detect this, and this may itself be a sufficiently distinctive descriptor to achieve the identification of intent, even if the tumbling makes actual imaging difficult.

1.3 | Sub-THz imaging

The high carrier frequencies of sub-THz radars allow wide-band signals to be generated easily, allowing the radar to achieve a range resolution of the order of centimetres. The cross-range resolution can easily be of the order of only 10 cm [6, 7]. In fact, for the simplest scheme, the same rule applies for the cross-range resolution as for the synthetic aperture radar, where, of course, it is the movement of the radar, rather than that of the target, which generates the Doppler shifts: The cross-range resolution is approximately half the antenna width. For a sub-THz radar, the antenna width may be of the order of 30 cm, whereas for lower-frequency radars, such small apertures give insufficient gain to effectively focus the transmitted signal. Even better cross-range resolutions can be achieved by tracking the object in bearing.

Another significant benefit of using a carrier frequency in the sub-THz band is that the wavelength becomes comparable to the surface roughness so the reflections become more diffuse than at lower frequencies. This makes the ISAR images more like optical images than those seen by radars operating at lower frequencies. The returns thus become more sensitive to variations in a surface texture which provides extra information to aid the recognition of features on the object.

The roughness of the surfaces has the additional benefit that it also reduces the reflectivity of the brightest parts of the image, thereby also reducing the overall dynamic range of the image and making it easier to avoid the 'dazzle' which can sometimes degrade such imagery.

As the authors in Refs. [6, 7] discussed the feasibility of the overall system design and image formation, this paper will look in more detail at the later stages in the processing scheme: creation of models of descriptors, using those models to recognise descriptors of the object and to estimate intent from those descriptors.

1.4 | Other work on the analysis of ISAR images of satellites from space

Other researchers [8, 9] have also recently discussed using ISAR to image objects in space using radars mounted in space, although they appear specifically to restrict themselves to the imaging of satellites, rather than space debris, spacecraft on extra-terrestrial missions or other objects. Their work simulates radars operating at Ku and X bands respectively, rather than the sub-THz frequencies assumed for the sensor in our work. The authors in Ref.[8] look at estimating the size and attitude of the satellite from observing its ‘capsule’ (presumably its body), rather than the solar arrays or other ‘descriptors’ which we use. It uses Deep Learning to teach it how to separate the body from the other descriptors. It uses iterative optimisation to find parameters which best fit the images. The authors in Ref. [9] similarly uses a deep neural network to ‘tidy up’ the images and uses this to separate the ISAR image characteristics created by the shape of the satellite from the Doppler produced by its internal motion so that its attitude and spin can be estimated. Although not mentioned in the title of [9], it uses bistatic imaging in order to estimate the complete motion. As noted above, the attitude and spin are used as inputs at the system level to our intent estimation process. These papers, however, do not discuss the recognition of the ‘discriminators’ nor the use of the images either to estimate either the identity of the satellite or its intent.

1.5 | System Architecture

The complete processing chain for the proposed sensor system is summarised in the flow chart shown in Figure 1.

The first stage is the radio-frequency signal generation and reception. One of our previous papers [6] concentrated on this aspect of the system, so it will not be described further here. The output of this first stage is transformed into coherent range profiles by the matched filter, and the Doppler information contained in these is converted to ISAR (range and cross-range) images using essentially known techniques but modified to suit the very high-range resolution of the sub-THz data. Again, this stage of the chain has been described in Ref. [6], and also in Ref. [7], and so does not need to be discussed in detail in this paper.

The next stage in the processing is to segment the ISAR images to separate specific features which can be identified and so provide the descriptors which can be used to estimate the intent of the object. This process is discussed briefly in section 2, and the feature set used in this work is described in section 3. The feature recognition process requires a training ‘library’ of reference features, and the ISAR images of which are created by electromagnetic modelling (EM) are also described in section 2.

Following the recognition of the features, the next stage is to estimate the intent from these features, and the processes

for doing this are described in section 4. Two approaches have been explored. The first approach is an expert system driven by human expert knowledge of the relationship between the descriptors and the object's intent. The second is a Bayesian scheme driven by prior observations of the probabilities of particular descriptors occurring on satellites with a particular intent.

The block diagram shows both methods being used in parallel with a final stage fusing their results. Whether both would actually be used, and if so how their estimates would be fused, are design decisions which will actually be made later in the development of the processing. These decisions will be informed by the results of experiments on the different estimation schemes described in section 4.

Note that the estimation schemes work purely on the descriptors (features) associated with the ISAR images. As mentioned above, there is a lot of other information which can be used to help with the process, such as the object's kinematics, its orientation, whether it is rolling etc. (see for, example [8–10].) In this diagram of the processing, this information is shown to be included at the last stage of the processing.

In the final system, all these processes would be carried out automatically, but in order to be able to start to investigate the components of the later stages of the work in parallel with the development of the earlier stages, for the purposes of this work, the extraction of the features from images was performed by eye.

2 | FEATURE RECOGNITION

2.1 | Feature modelling'

Most methods of recognising descriptors in images require training data. This is clearly not available for objects which are new and ‘unknown, that is, which have not been seen before, hence the need to recognise their intent by recognising their descriptors rather than recognising the whole object. We cannot gather training data on the complete set of possible descriptors, or look for angles on the object which are not available from Earth. It is therefore very important that we should be able to use electromagnetic modelling (EM) to create the training data which will allow us to recognise individual descriptors.

The approach proposed for this work is to use a hybrid method of Geometrical optics (GO) and Physical optics (PO). Geometrical optics is a high-frequency approximation of Maxwell's equations, useful for simulating the propagation of EM waves through large structures. It is computationally efficient but may not accurately model the detailed interactions between EM waves and small structures. This weakness is addressed by the integration of PO into the model. Physical optics models electromagnetic waves as a combination of incident and scattered waves and uses Kirchhoff's integral theorem to compute the scattered field.

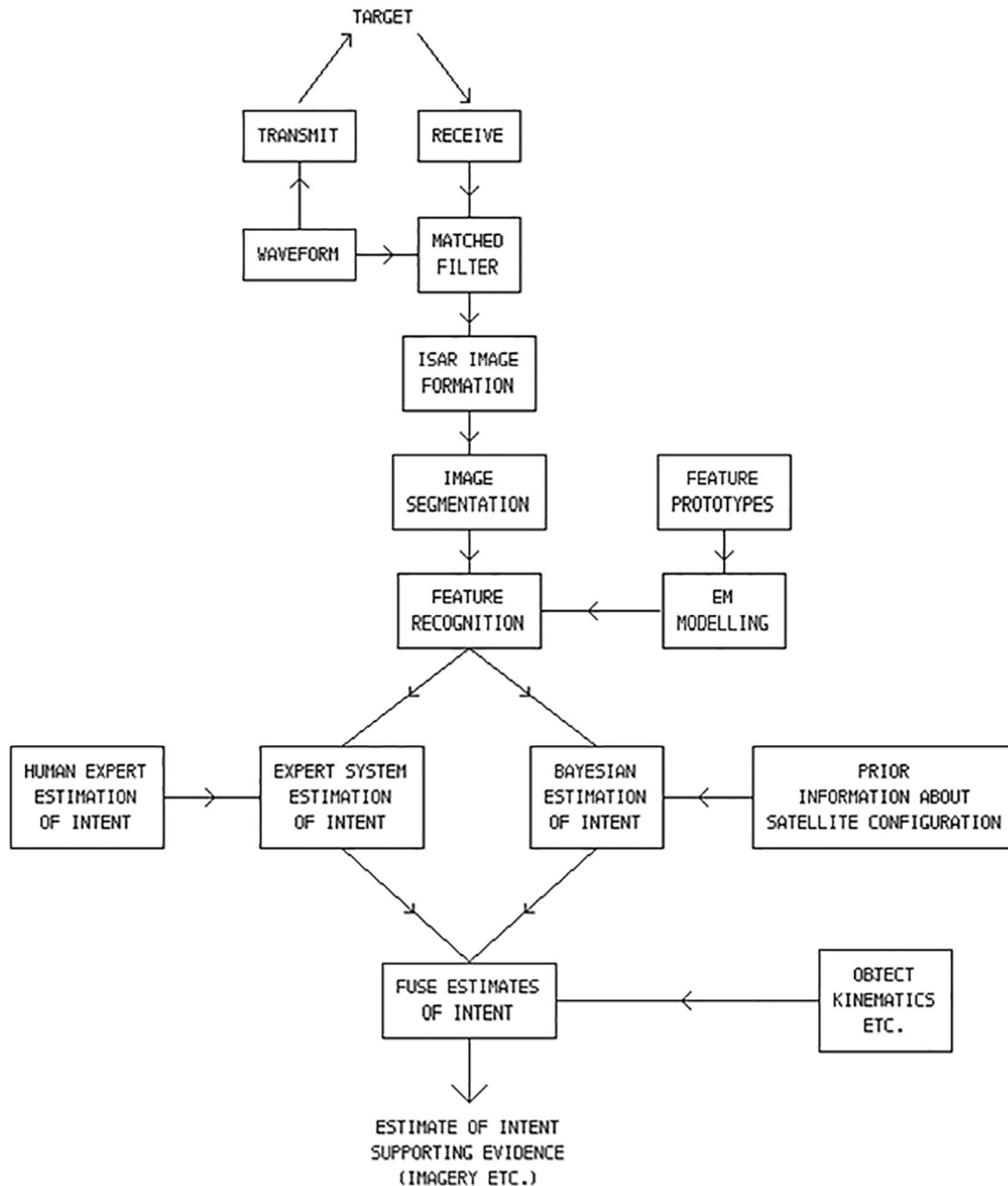


FIGURE 1 System architecture.

Ray-tracing algorithms which are used to implement the principle of GO require the object and the wavefronts to be sampled with a resolution of at least half a wavelength. As a result to reconstruct the scattering of a large target such as a satellite, the dimensions of which can be in the order of tens of metres, at sub-THz frequencies, the number of calculations required for the first ray/face intersection is in the order of several millions, and this number increases when multiple scattering mechanisms are considered. Additional processing is also required to remove the contribution from shadowed target areas and, therefore, the identification of illuminated and shadowed regions on the geometrical model of the target is a complex problem. Classical techniques for ray optics calculations often therefore use approximations which can reduce the accuracy of the scattering calculation.

To overcome these limitations, 3D computer graphics software tools can be used to obtain an image of the target based on the ray-tracing calculation, including multiple bounces and, if the viewpoint of the target is located at the position of a monostatic radar aperture, the result of calculations contains only the illuminated surfaces, shadowed ones being removed [11]. Blender [12] has been selected as an appropriate platform to perform the ray-tracing calculations. It propagates rays back from the image plane to the light source via reflections from the object. For radar modelling, the image plane corresponds to the location of the receiver, and a distributed light source emulates the wavefront incident on the target. Blender also gives the depth information needed to add target range information onto the data.

2.1.1 | Surface roughness model

To model rough surfaces, Blender uses the Oren–Nayar reflectance model [13] which predicts the reflectance from rough surfaces. The surfaces are modelled as a set of facets having different slopes. The roughness is specified by the standard deviation of the slopes of the facets, which are assumed to have a Gaussian distribution.

Figure 2 shows the image of a sphere at 300 GHz and at 75 GHz with the same roughness. It clearly shows that at 300 GHz, the scattering is predominantly diffused so the shape and size of the sphere can be seen, while at 75 GHz, the reflection comes only from the sections of the spherical surface which are approximately perpendicular to the incoming rays, giving specular scattering.

2.2 | ISAR simulations

The output of the EM modelling can be used to create ISAR images of features which can be used to train the feature recognition system.

The simulation is made following the steps:

1. Determination of range and cross-range resolutions and relative radar bandwidth and integration angle
2. Frequency vector generation
3. Generation of the azimuth angle of the radar at each pulse (integration angle step)
4. Calculation of the position of the target at each pulse relative to the radar
5. Calculation of the differential range of each scatterer of the target relative to the radar
6. Update the phase history for each step angle
7. Range-Doppler processing of the phase history vector to form the image.

More details of the ISAR image formation are given in Ref. [7].

Figure 3 shows a Computer-Aided Design (CAD) model of the satellite Calipso [14].

The model of the body has dimensions of 2.46 (height) \times 1.51 \times 1.91 m, and the solar panels extend the

width dimension to 4 m, and the total area of the satellite is ~ 11.5 m². The wavefront is sampled at 1/10th wavelength spacing at 300 GHz.

Figure 4 shows the equivalent scattering model and the ISAR image at 300 GHz.

Figure 5 shows the ISAR image of a solar panel at 75 GHz and at 300 GHz as an example of a feature in which the system would need to recognise.

The authors in Ref. [6] also discuss EM simulation at sub-THz frequencies, although the approach used there did not make use of Blender. The authors in Ref. [7] show examples of ISAR images of discriminant features measured in the laboratory.

2.3 | ISAR image segmentation

Sections of the satellites which can be used to produce a set of discriminants can be isolated directly from the high resolution ISAR images using image processing techniques such as image segmentation. A good technique for achieving this is Statistical Region Merging [15]. This is a fast and robust algorithm to segment an image into regions of similar intensity. The method involves iteratively merging adjacent image regions based on a statistical criterion, such as similarity of pixel values or texture features and is particularly used for images with homogenous regions or having low contrast, where edge detection is

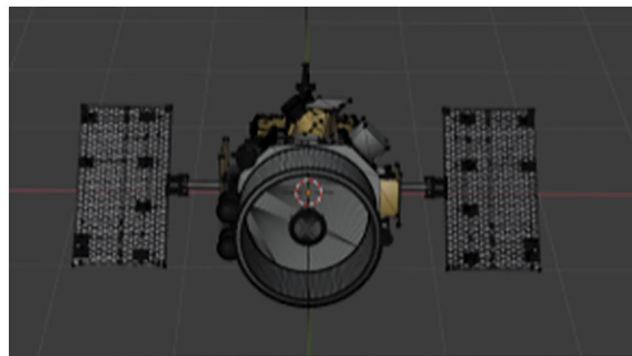


FIGURE 3 Computer-Aided Design (CAD) model of Calipso.



FIGURE 2 Rendered images of a rough sphere at 300 GHz (a) and 75 GHz (b).

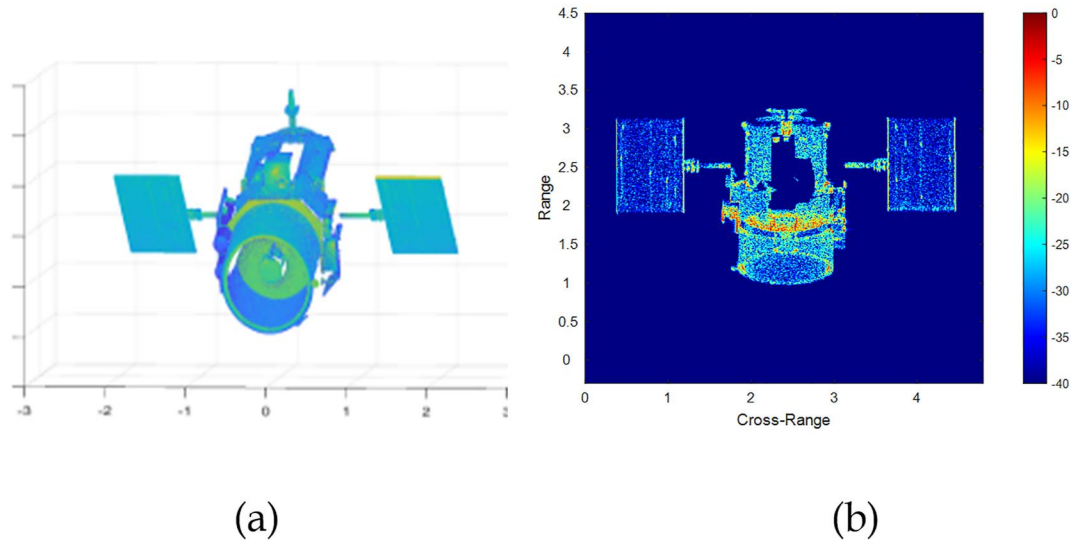


FIGURE 4 (a) Scattering model (b) an Inverse Synthetic Aperture Radar (ISAR) image of Calipso at 300 GHz.

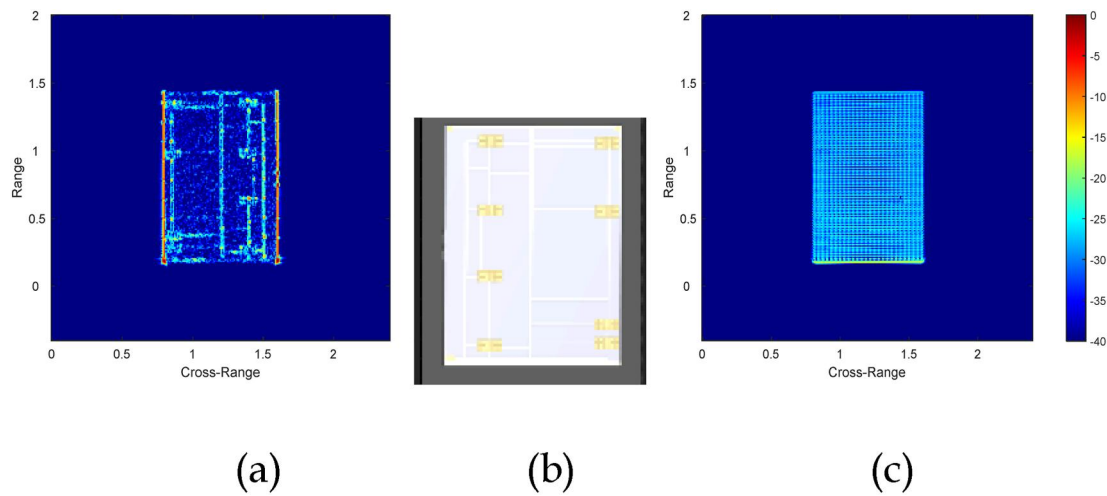


FIGURE 5 Inverse Synthetic Aperture Radar (ISAR) image of the solar panel satellite at 300 GHz (a) and 75 GHz (c) with 1 cm^2 resolution. (b) Computer-Aided Design (CAD) model of the solar panel.

difficult. An example of the segmentation method applied to an ISAR image of the satellite Inmarsat-4 is shown in Figure 6.

The ISAR image is first smoothed and then segmented. The superpixels thus obtained are able to segment the image (Figure 6b) into three regions corresponding to the satellite body, the solar panels and the large circular reflector above the body.

A second level of segmentation is then applied to the satellite body of which a model and the ISAR image are shown in Figure 7.

To show the capability of the segmentation method to recognise the damage on satellites, an exposed piece of the honeycomb panel has been placed on the front of the satellite body to represent damage—it is visible on the lower left of the model and of the ISAR image.

The ISAR image is segmented again using an increasing level of detail, as shown in Figure 8. The result is an increasing number of superpixels segmenting the image with smaller sizes.

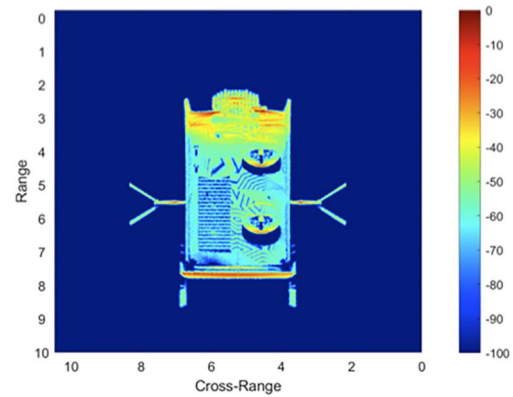
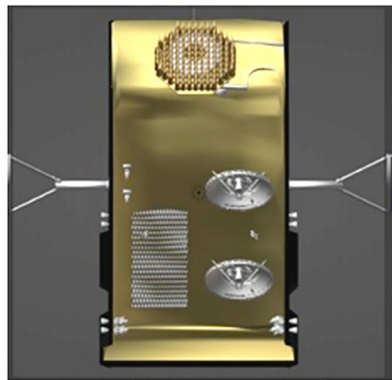
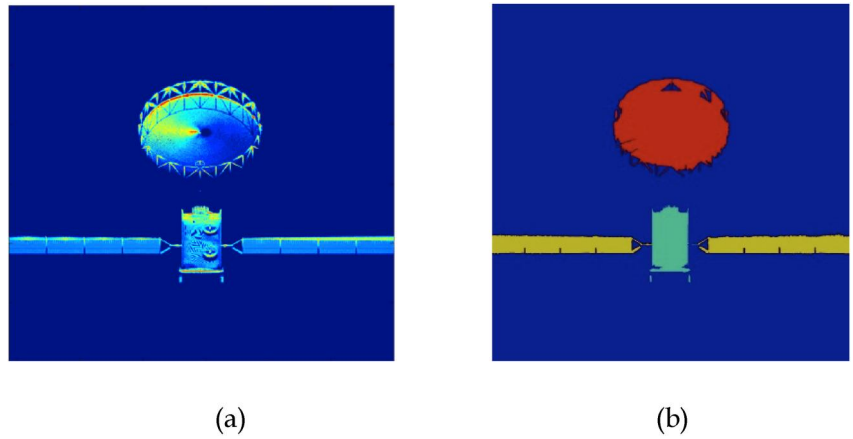
These are able to isolate single features of the satellite body, such as the array antenna feed on the top or the small antenna dishes on the left, as well as the piece of the exposed honeycomb panel.

The final stage of the feature recognition will be for each superpixel of the segmented image to be labelled based on a comparison of its appearance with the isolated features as obtained from the EM.

3 | DESCRIPTOR SET

The set of descriptors found by the image segmentation can then be used to estimate the intent of the object. The complete set of descriptors which needs to be recognised has been derived by considering those on different objects found in space. Different researchers may create slightly different sets,

FIGURE 6 Inverse Synthetic Aperture Radar (ISAR) image (a) and segmentation with the single degree of complexity (b) of the Inmarsat-4 model.

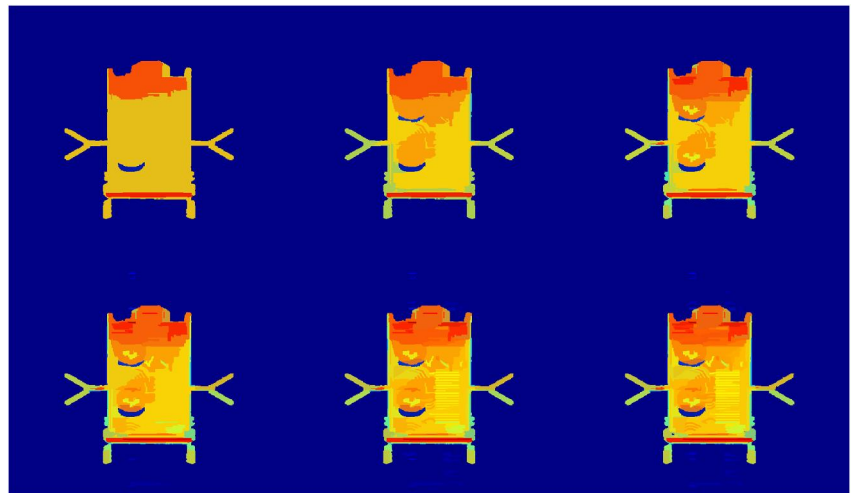


(a)

(b)

FIGURE 7 Model (a), Inverse Synthetic Aperture Radar (ISAR) image (b) of the Inmarsat satellite body with a piece of the exposed honeycomb panel.

FIGURE 8 Segmentation of the Inmarsat satellite body Inverse Synthetic Aperture Radar (ISAR) image with the increasing degree of complexity.



and an operational system would have to have a descriptor set which is the union of those created by different researchers. The set we used will, however, serve as an example of how the process works. This is listed in Table 1.

Some of these descriptors are directly indicative of intent, such as (large) telescopes and large radio frequency antennas. Others, such as the type of thruster may be indirectly indicative, for example, by suggesting how much maneuvering the

object is expecting to undertake. Sometimes combinations can be indicative of intent, for example, a large antenna array may indicate a communications satellite, but if that is indeed its intent, it should also have large solar arrays to provide the power for the transmitters.

Although the primary need is to recognise the intent of unknown objects, the processing can easily be modified to recognise known objects from their descriptor sets. This is not normally necessary since the ephemeris data and existing tracking networks will know the objects' identities from their positions in space, but it could be useful in two cases: when an unknown object turns out to be of the same design as a known one and when a known object has been damaged or 'upset' (rotated) and is therefore in an unexpected orientation in which the recognition system can detect. This will be a reason for also recognising descriptors such as star trackers or patch antennas, which may not be so distinctive of intent.

3.1 | Missing Descriptors

Another significant case is where the object does not have any obvious solar cells or radio frequency antennas. The objects which would come into the category of 'Missing Descriptors' are listed in Table 2:

TABLE 1 Set of descriptors.

Array antenna
Boom
Chemical thruster
Cold gas thruster,
Conical horn
Hall effect thruster,
Helical antenna
Lidar
Monopole
Patch array
Pyramidal horn
Reflector
Solar array
Solar array on the body
Star tracker
Telescope

TABLE 2 Objects with missing descriptors.

Missiles
Dead boosters in orbit
Severely damaged satellites

Note that in conventional usage, Dead Boosters and Damaged Satellites are classified together as 'large space debris.'

Space craft which have no antennas may also fall into one of these categories or else perhaps be space craft on completely autonomous missions which will then be physically recovered. An example of such a mission would be sampling the solar winds, such as [16].

Space craft which have no solar panels would also probably be either in the 'Missing Descriptor' class or else be on missions to the outer Solar System where the sunlight is weak and which may, perhaps, be nuclear-powered.

Space craft with either no antennas or no solar panels should be referred to human analysts for further investigation, as, of course, should anything which appears to be particularly unusual or suspicious.

3.2 | Damage as a discriminator

As discussed above, one reason why a satellite may have no solar panels or no antennas could be that it is damaged. Damage may also be recognised at the descriptor-recognition stage, either as an unrecognised, probably irregular, descriptor or as an anomaly in a recognised descriptor, such as gaps in the regular pattern of the sections of a solar array. If the descriptor recognition identifies 'damage', then of course, this can trivially be noted in the estimate of its intent.

4 | ESTIMATION OF INTENT

An experimental study was made of the process of estimating intent from the descriptors.

4.1 | Expert system

The primary approach to estimating intent was to use an expert system approach [17], whereby human experts frame rules which are used to estimate intent, and these are programmed into a computer programme. The rules were of the form:

If the object has a boom then its intent is probably science (the boom probably keeps a sensor away from the object's body).

If the satellite has array antennas then its intent is probably either Earth Observation, Space Observation Communications, Broadcasting, Space Probe Communications or Weather Research.

If the satellite has a large telescope then its intent is probably Earth Observation or Space Observation.

If it has a SAR antenna its function is SAR earth observation.

Note that this approach, at least as implemented, makes little use of the information which is available about the size of the descriptors and no use of the information about their locations, as these factors are of little value if the a priori identity of the satellite and hence the expected size and locations of the descriptors are unknown.

The rules were quantified by creating an array of real numbers, one for each of the possibilities in Table 1, representing how likely it was that that was the object's intent. The rules illustrated above were thus coded as follows:

```

if  $N\_Of$  [Boom > 0 then
    Inc (P [ Science ], 1);
if  $N\_Of$  [Array_Antenna > 0 then
begin
    Inc (P [ Earth_Observation ], 1);
    Inc (P [ Communications ], 1);
    Inc (P [ Broadcasting], 1);
    Inc (P [ Space_Probe_Comms], 1);
    Inc (P [ Weather_Research], 1);
    end;
if ( $N\_Of$  [Telescope > 0] and ( $Area\_of$ 
    (Telescope,  $S\_F$ ) >  $Body\_Area$  ( $S\_F$ .Body) / 2)
then
begin
    Inc (P [ Earth_Observation ], 1);
    Inc (P [ Space_Observation ], 1);
    end;
if (P[SAR > 0] then
    if Long_Antenna ( $S\_F$ ) then
        Inc (P[SAR], 0.3);
    else
        Dec (P[SAR], 0.3);

```

Where N_Of is an array containing the number of examples of each descriptor type found on the image, *Inc* and *Dec* are procedures to add and subtract a number from the array, P , mentioned above, representing the likelihood that the object has any specific intent. *Area_of* is a procedure which estimates the size of a discriminator, *Body_Area* is an estimate of the size of the body of the object and *Long_Antenna* determines whether the antenna has one dimension significantly longer than the other, which indicates that it is probably a SAR antenna. S_F is the set of discriminators found on the object.

Once all the rules have been applied, the algorithm returns the intent which has a highest p -value.

4.1.1 | Test data

As noted above, the representative test data could not be obtained from observing real satellites, also in this experimental stage not having a radar in orbit made it completely impractical. Because the research into the estimation of intent was done in parallel with the development of the modelling

and the descriptor recognition, modelled data could not be used either.

The data base was therefore created from visual images of space objects from which the identities, sizes and positions of the descriptors were measured by hand by scaling the images. Although these may not be particularly accurate representations of the descriptor sets of the objects of which we had images, they were self-consistent and representative of real objects. A set of 67 objects was used, with an average of just over 5 descriptors per object. The set of intents of these objects is listed in Table 3.

'Observation' refers to both Earth observation and observation of deep space, since the main difference between them is whether the sensor is directed, broadly speaking, upwards or downwards. The recognition of the intent process cannot distinguish between these cases but, of course, the estimate of the object's attitude which is also obtained from its image will be able to resolve this. 'Exploration' is short for space exploration in general, such as travelling to and observing other planets. 'Science' covers other scientific experiments, such as observing the solar wind. 'ELINT' is an abbreviation for Electronic Intelligence, that is, listening to signals, particularly military signals, such as radar and communications, which are emitted from the Earth.

No attempt was made to equalise the number of objects in each category since the relative numbers are probably a fair representation of the proportion of objects in each category in orbit.

Figures 9 and 10 illustrate how the set of discriminators corresponding to each object was derived. Figure 9 shows an image of the Ikonos satellite, and Figure 10 shows how the discriminators were identified from this image.

The process is essentially the same as that described above for segmentation of the ISAR images except that it is carried out 'by eye' on a visual image rather than automatically on an ISAR image. Information about the size of the satellite, in this

TABLE 3 Set of intents of objects in the data base.

Intent	Number of Examples
Observation	28
Exploration	17
Science	6
Communications	4
Broadcasting	2
Spacecraft	2
Space station	2
SAR	2
ELINT	2
Missile	1
Retrieval	1

Abbreviations: ELINT, electronic intelligence; SAR, synthetic aperture radar.



FIGURE 9 The Ikonos satellite (credit: Turbosquid).

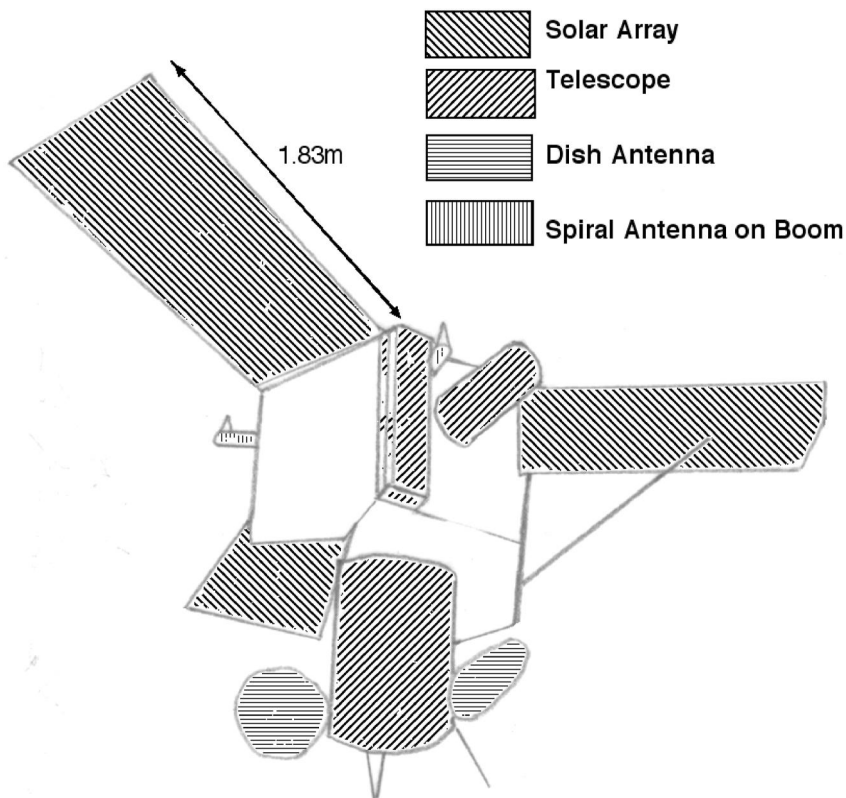


FIGURE 10 Discriminants identified on the image of Ikonos.

case the length of the solar arrays, was obtained from Wikipedia, which allowed the set of discriminants to be scaled. When estimating, their size account was taken from the perspective of the visual image, although this was only done

approximately. The key point is, again, that the data is self-consistent and representative of a real satellite, even if it is not a highly accurate representation of the actual Ikonos satellite.

When testing the process, it should be noted that not all the descriptors on an object will be visible from any one aspect angle. A sophisticated approach in tackling this would be to use CAD models of all the objects in the data set and determine how many of its descriptors could be seen from each aspect angle and then to perform the estimation of intent for each object at a large number of aspect angles. For a first look, however, it was decided that the process could be simplified by performing the estimation once for each object using a randomly-chosen subset of its descriptors. For the experiment, 50% of the descriptors on the object were used.

The experiment was also repeated using all the descriptors, and it was shown that taking only half of them did not significantly affect the results, suggesting that the approach used is reasonably robust.

Table 4 shows a representative confusion matrix produced by the expert system.

Each row represents the estimates of the Intent of each satellite of each type, so each column represents the number of satellites of each type which were estimated to have a given Intent.

At first glance, the confusion matrix shows only modest performance, when it was considered that observation satellites were the most common in the data set. The number of satellites the Intents of which were identified correctly was 12 (19%).

4.2 | Bayesian approach

Bayes' rule can be expressed as follows:

$$p(\text{intent}|\text{descriptor}) = \frac{p(\text{descriptor}|\text{intent}) \times p(\text{intent})}{p(\text{descriptor})}, \quad (1)$$

where $p(\cdot)$ represents a probability. This means that knowing the observed probabilities of descriptors appearing on an object, we can deduce the probability that it has a particular intent. The usual problem with the Bayesian analysis is in obtaining the prior probabilities, in this case $p(\text{intent})$ and $p(\text{descriptor})$. The 'closed' data set which was created to test the 'expert system' approach also gave use the data set which could be used to perform a Bayesian estimation, since we had the complete 'ground truth,' so the Bayesian approach became practical in this case, even though providing the prior probabilities might be a problem for a real system.

This approach was implemented separately for each type of the descriptor seen on each object by calculating the value of $p(\text{intent}|\text{descriptor})$ derived from Equation (1) using the values of $p(\text{descriptor}|\text{intent})$ and $p(\text{intent})$ derived from the full data set, with $p(\text{descriptor})$ being set to 1. The values of $p(\text{intent}|\text{descriptor})$ obtained for each intent for each descriptor type were all added together for each object, giving an array of the probabilities that the object had each possible intent. The summation is a naïve process since it assumes that the probabilities that each descriptor type is present on an object are independent, that is, it takes no account of the probability that if one descriptor type is present, another is also likely to be present. It also takes no account of the number of examples of that descriptor or of their sizes or positions.

The Bayesian approach allows one to consider more than then the single 'most likely' class, including the second choice that significantly increases the proportion of correct estimates. The algorithm thus returned both the intent with the highest probability and also that with the second highest probability. This approach is not well expressed by a conventional confusion matrix, but Table 5 shows the number of correct estimates for the first choice and within the first and second choices.

This gives a total of 38 correct estimates (57%).

TABLE 4 Confusion matrix for the expert system.

Truth	Estimate										
	Obs.	Explore	Sci	Comm	B'cast	S/craft	S/Stn	SAR	ELINT	Missile	Retrieval
Observation	8	0	1	4	0	0	0	0	1	0	0
Exploration	2	0	2	4	0	0	0	0	0	0	0
Science	0	0	2	0	0	0	0	0	0	0	0
Communications	0	0	0	2	0	0	0	0	0	0	0
Broadcasting	0	0	0	1	0	0	0	0	0	0	0
Spacecraft	0	0	0	1	0	0	0	0	0	0	0
Space station	0	0	0	0	0	0	0	0	0	0	0
SAR	0	0	0	1	0	0	0	0	0	0	0
ELINT	0	0	1	1	0	0	0	0	0	0	0
Missile	0	0	0	0	0	0	0	0	0	0	0
Retrieval	0	0	0	0	0	0	0	0	0	0	0

Abbreviations: ELINT, electronic intelligence; SAR, synthetic aperture radar.

TABLE 5 List of correct first and second estimates—Bayesian estimates.

Intent	Number Correct	
	1 st Choice	2 nd Choices
Observation	9	13
Exploration	0	1
Science	3	0
Communications	2	0
Broadcasting	1	0
Spacecraft	1	1
Space station	0	1
SAR	2	0
ELINT	2	0
Missile	1	0
Retrieval	1	0

Abbreviations: ELINT, electronic intelligence; SAR, synthetic aperture radar.

Once again, the result is for the case where only half the descriptors are visible, but the results were not significantly different for the case where all the descriptors were assumed to be visible.

One notable positive feature of these results is that the Bayesian approach is very good at recognising the more ‘unusual’ classes (SAR, ELINT, Missile and Retrieval), albeit their overall rarity means that there is a proportionately high false alarm rate for these classes. It may be noted that detecting these ‘unusual’ classes is probably more valuable than identifying the more common classes.

One disappointing aspect of these results is the inability of either the Bayesian or the Expert System approaches to recognise space Exploration craft.

4.3 | Recognition of identity

As discussed above, the recognition of identity is a useful capability to add to the system for cases where an unknown object is found to be of the same class as a known object or where a known satellite has been damaged.

When an estimate of the identity of the object is made based on its complete descriptor set, it was quite easy to correctly identify all 67 objects in the data set, that is with no erroneous matches and no failures to match the object to the data set. With a more realistic case where half the descriptors (again chosen at random) were visible, 10 cm r.m.s uncertainty was added to the estimates of the sizes and positions of the descriptors, and the classifier had tolerances that 30% of the descriptors had to be recognised and their sizes and positions had to match within ± 0.5 m, and 63 of the objects (94%) were still recognised correctly.

5 | CONCLUSIONS

This paper has described the structure of a system for recognising the intent of objects based on recognising the descriptors in their ISAR images, as measured by a space-based sub-THz radar.

The first step of this approach is to recognise the descriptors and the paper has discussed how a suitable set of ISAR images can be created by simulation to train the recogniser. This must be done by simulation since it is impractical to gather enough training data on real objects in space.

The second step is to deduce the intent from the set of descriptors. An initial set of descriptors and a set of intents have been deduced from a priori knowledge and from observing images of satellites, and these have been tabulated in the paper.

The deduction of intent from descriptors has been performed using an expert system. The test data for this has been obtained from ‘optical’ images of the satellites as a surrogate for a completely developed descriptor recognition system.

An alternative Bayesian estimation approach was also tested using the same data base. The latter gave better results, providing 57% correct estimation when it was allowed to return two estimates. It was particularly good at recognising unusual classes and therefore shows promise of being a useful aid to reduce the workload on human analysts.

It is important to note again that the final stage in the identification of intent will combine the estimate based on the descriptor set, which has been examined here, with other information, such as the object's ephemeris, its aspect (which can resolve, for example, whether it is observing the Earth or other celestial objects) and its internal motion.

A secondary experiment, to find out whether ‘known’ satellites could be identified from their descriptors, was very successful showing very good and very robust results, being able to cope with errors of at least 10 cm in the estimates of sizes and positions of the descriptors. This capability could in practice be used to recognise new satellites which were of the same class as known satellites, or, alternatively, which were not what they claimed to be, or satellites which were out of position.

Estimating intent from the features on the object opens the way to a deception technique of adding extra ‘features’ to an object to disguise its true intent. This, however, has two potential problems: one is that it is always expensive to add extra features onto something being launched into space, so this option is not cost-free. The second problem is that if the intent implied by the spurious features is incompatible with what can be deduced from the kinematic and other information that in itself becomes an indication that a deception is being attempted.

AUTHOR CONTRIBUTIONS

Andrew Gerald Stove: Conceptualisation; funding acquisition; investigation; software; writing – original draft; writing – review & editing. **Marina Gashinova:** Conceptualisation;

funding acquisition; methodology. **Edward Hoare**: Conceptualisation; investigation; resources; supervision; validation; writing – original draft. **Mikhail Cherniakov**: Conceptualisation; funding acquisition; supervision; writing – review & editing. **Emidio Marchetti**: Conceptualisation; data curation; investigation; software; writing – original draft.

ACKNOWLEDGEMENTS

The expert system rule set and the set of descriptors are based on the information provided by Jack Booth of Airbus Defence and Space Ltd. This work was funded by the Defence Science and Technology Laboratory, United Kingdom, as part of the Defence and Security Accelerator competition under the “Multi-Dimensional ISAR Imagery From Space To Space” project (MARS), contract DSTLX1000163770.

CONFLICT OF INTEREST STATEMENT

The authors have no conflicts of interest associated with this work.

DATA AVAILABILITY STATEMENT

The research data are not shared.

ORCID

Andrew G. Stove  <https://orcid.org/0000-0002-1443-1202>

REFERENCES

- Ender, J., et al.: Radar techniques for space situational awareness. In: 12th International Radar Symposium (IRS), pp. 21–26. Leipzig (2011)
- Lal, B., et al.: Global trends in space situational awareness (SSA) and space traffic management (STM). In: IDA Science & Technology Policy Institute. IDA Document D-9074 Log: H 18-000179, Washington (2018)
- Pillai, S.U., Li, K.Y., Hamed, B.: Space Based Radar: Theory & Applications, pp. 77–97. McGraw Hill, New York (2008)
- Benson, C.R.: Enhancing space situational awareness using passive radar from space based emitters of opportunity. In: 2014 Military Communications and Information Systems Conference (MilCIS), pp. 1–5. Canberra (2014)
- Anger, S., et al.: ISAR imaging of satellites in space – simulations and measurements. In: 2019 20th International Radar Symposium (IRS), pp. 1–6. Ulm, Germany (2019)
- Marchetti, E., et al.: Space-based sub-THz ISAR for space situational awareness—concept and design. In: IEEE Transactions on Aerospace and Electronic Systems, vol. 58, pp. 1558–1573 (2022)
- Marchetti, E., et al.: Space-based sub-THz ISAR for space situational awareness - laboratory validation. In: IEEE Transactions on Aerospace and Electronic Systems, vol. 58, pp. 4409–4422 (2022)
- Wang, J., et al.: Attitude and size estimation of satellite targets based on ISAR image determination. IEEE Trans. Geosci. Rem. Sens. 60, 1–15 (2022). <https://doi.org/10.1109/tgrs.2021.3139962>
- Zhou, Y., et al.: Automatic dynamic estimation of on-orbit satellites through spaceborne ISAR imaging. IEEE Trans. Radar. Sys. 1, pp34–45 (2023). <https://doi.org/10.1109/trs.2023.3267739>
- Marto, S.G.O., et al.: Multi-static radar for manoeuvre detection. In: IET Conference Proceedings, pp. 160–165 (2022). <https://doi.org/10.1049/icp.2022.2309>
- Rius, J.M., Ferrando, M., Jofre, L.: GRECO: graphical electromagnetic computing for RCS prediction in real time. In: IEEE Antennas and Propagation Magazine, vol. 35, pp. 7–17 (1993)
- <https://docs.blender.org/>
- Oren, M., Nayar, S.K.: Generalization of Lambert's reflectance model. In: Proceedings of the 21st Annual Conference on Computer Graphics and Interactive Techniques (1994)
- <https://nasa3d.arc.nasa.gov/models>
- Nock, R., Nielsen, F.: Statistical region merging. In: IEEE Transactions on Pattern Analysis and Machine Intelligence, vol. 26, pp. 1452–1458 (2004)
- <https://curator.jsc.nasa.gov/genesis/>. at 10:45 GMT. Retrieved 16 June 2023
- Waterman, D.A.: A Guide to Expert Systems Waterman. Reading. Addison-Wesley (1986). ISBN 978-0-20108-313-2

How to cite this article: Cherniakov, M., et al.: Recognition of objects in orbit and their intentions with space-borne sub-THz Inverse Synthetic Aperture Radar. IET Radar Sonar Navig. 1–13 (2023). <https://doi.org/10.1049/rsn2.12513>